

Supporting Information

Equipment-free photothermal effect promoted self-healing and self-recovery of hydrogels

Xinjie Zhang,^{‡a} Xuechen Liang,^{‡ab} Qichen Huang,^a Han Zhang,^b Changkun Liu^a and Yizhen Liu^{*a}

^a College of Chemistry and Environmental Engineering, Shenzhen University, Shenzhen 518055, China. E-mail: yzliu@szu.edu.cn

^b Key Laboratory of Optoelectronic Devices and Systems of Ministry of Education and Guangdong Province, College of Optoelectronic Engineering, Shenzhen University, Shenzhen 518060, China.

[‡]These authors contribute equally to this work.

List:

1. Experimental section

1.1 Materials

1.2 Synthesis

1.2.1 Microgels

1.2.2 C/P(AAm-AAc)/Fe³⁺ hydrogel

1.2.3 PDA

1.2.4 PVA/PDA/Borax hydrogel

1.3 Characterizations

1.3.1 Mechanical properties

1.3.2 Self-healing

1.3.3 Photothermal performance test

Fig. S1 Synthesis diagrams: (a) C/P(AAm-AAc)/Fe³⁺, (b) the cross-linking mechanism of C/P(AAm-AAc)/Fe³⁺ hydrogel, (c) PVA/PDA/Borax hydrogel.

Fig. S2 (a) Swelling curves of C/P(AAm-AAc)/Fe³⁺ hydrogels swelled in different solvents and (b) digital photos after swelling for 140 h.

Fig. S3 The temperature rises of PVA/PDA/Borax and C/P(AAm-AAc)/Fe³⁺ hydrogels under simulated sunlight.

Fig. S4 The actual sunlight irradiation intensity during wound self-healing test: (a) PVA/PDA/Borax hydrogel, (b) C/P(AAm-AAc)/Fe³⁺ hydrogel.

Fig. S5 Effect of immersion time in FeCl₃ of 0.05 mol/L on mechanical properties of C/P(AAm-AAc)/Fe³⁺ hydrogel: (a) original sample, (b) self-healed sample.

Fig. S6 (a) The tensile stress-strain curves of as-prepared C/P(AAm-AAc)/Fe³⁺ hydrogel and self-healing cut-in-two C/P(AAm-AAc)/Fe³⁺ hydrogel at different times under simulated sunlight. (b) The self-healing of C/P(AAm-AAc)/Fe³⁺ hydrogel under room temperature, 55 °C oven and simulated sunlight for 6 h.

Fig. S7 The tensile fracture curves of the original sample, the cut-healed once sample, and the cut-healed five times sample: (a) PVA/PDA/Borax hydrogel (Borax: 3.0%; PDA: 1.5%; F-T-3; healing time: 3 h), (b) C/P(AAm-AAc)/Fe³⁺ hydrogel (healing time: 6 h).

Table S1 The collations and comparisons of self-repair research results reported in the literature compared from materials, healing mechanisms, healing conditions, efficiency and speed of self-healing and published years.

1. Experimental section

1.1 Materials

Polyvinyl alcohol 1799 (PVA), broax, ammonia water ($\text{NH}_3\text{-H}_2\text{O}$), anhydrous ethanol, 2,2,3,4,4,4-hexafluorobutyl methacrylate (HFBMA), sodium dodecanesulphonate (SDS), *N,N'*-methylene-bis-acrylamide (MBA), acrylic acid (AAc), ammonium persulphatesodium (APS), hydrochloric acid (HCl), carbon powder, ferric chloride (FeCl_3) were purchased from Aladdin Reagent, China. Dopamine hydrochloride was purchased from Meryer, China. Allylamine (AA) was purchased from Shanghai Rhawn Reagent, China. They were all analytical and used as received. Acrylamide (AAM) was purchased from J&K Reagent, China and recrystallized from acetone and vacuum dried at 40 °C. Deionized water was used in all experiments.

1.2 Synthesis

1.2.1 Microgels. Microgels were prepared using the methods reported in the literature,¹ as shown in Fig. S1a. Taking the preparation of a total of 250 g of the microgel dispersion as an example, 11.458 g HFBMA and 0.188 g SDS were added to a three-necked flask, sonicated for 2 min, and then 0.099 g MBA and around 50 g water were added. Then weight 1.046 g AA in a small beaker, dilute with appropriate amount of water, and transfer to a three-necked flask. The total water mass was added to 228.550 g and sonicated for 2 min to obtain a turbid, slightly white heterogeneous reaction solution. The reaction was carried out in a 70 °C water bath. The mechanical agitation speed was 250 rpm. Oxygen was purged with nitrogen during the reaction. After 30 min, the polymerization reaction was initiated by adding a 14.700 g 1.5 wt% APS initiator solution. The reaction was continuously stirred for 6 h to obtain a milky white microsphere dispersion which was a 5 wt% solution of HFBMA microspheres.

1.2.2 C/P(AAm-AAc)/ Fe^{3+} hydrogel. Learned from the reported literature,¹ first, 11.154 g of AAm, 0.846 g of AAc, 0.600 g of carbon powder, and 48.000 g of a solid content of 5 wt% of the microgel solution were placed in a 250 mL conical flask and ultrasonically dispersed for several minutes. The pH of the reaction solution was adjusted to approximately 3 using an aqueous solution of 18 wt% HCl, followed by pumping, introducing nitrogen gas to remove oxygen in the system, and adding 4.110 g APS initiator of a solid content of 10 wt% under ice water bath. Next, the solution was transferred to airtight mold (plastic syringe or parallel plate mold made of two glasses and a silicone strip) and polymerized at 25 °C for 24 h to obtain the as-prepared C/P(AAm-AAc) hydrogels. The cross-linking mechanism is shown in Fig. S1b. Finally, the above hydrogels were immersed in a 0.050 mol/L FeCl_3 solution, and the C/P(AAm-AAc)/ Fe^{3+} hydrogels of different ion crosslinking degree were obtained by altering the immersion time.

1.2.3 PDA. Polydopamine particles were prepared by the method reported in the literature.^{2,3} The details are as follows: 4 mL ammonia water, 80 mL ethanol and 180 mL deionized water were mixed, and fully stirred at room temperature to make the solution A. Further, 1 g dopamine hydrochloride was dissolved in 20 mL deionized water and this solution was labeled B. The solution B was added to the solution A with stirring. The mixed solution quickly changed from colorless to yellowish brown and gradually turned dark brown. Stirring was continued for 12 h at room temperature. The reaction solution was centrifuged at 12,000 rpm for 15 min to collect the sediments. It was washed three times with deionized water and then dried in an oven at 60 °C to obtain the final black polydopamine nanoparticles powder, as shown in Fig. S2a.

1.2.4 PVA/PDA/Borax hydrogel. As shown in Fig. S1c, first, a certain amount of PDA was dispersed in 100 mL deionized water under ultrasound. Then the PDA solution was heated to 90 °C and 20 g PVA was added with stirring to form a homogeneous PVA/PDA solution. Then a certain amount of borax was added to the above PVA/PDA solution to form a borax solution having a borax mass fraction of 4 wt%, and the mixture was stirred at 90 °C to be uniform. Next, the mixed solution was poured into airtight mold (plastic syringe or parallel plate mold made of two glasses and a silicone strip). After standing at room temperature for 2 h, the solution in the template was subjected to a sol-gel transition. It was then placed in a refrigerator at a freezing temperature of -20 °C for 2 h and then allowed to thaw at room temperature for 6 h. Finally, the above freeze-thaw process was repeated 2–4 times to prepare hydrogels of different freeze-thaw cycles. As shown in Fig. S2b, PVA/PDA/Borax hydrogel was successfully prepared, and the PDA particles were uniformly dispersed in it.

1.3 Characterizations

1.3.1 Mechanical properties. The tensile mechanical properties of PVA/PDA/Borax and C/P(AAm-AAc)/ Fe^{3+} hydrogels samples were tested using a universal testing machine (CMT4304, MTS, USA) at a test speed of 10 mm/min. The tensile fracture strength σ and fracture deformation ε are calculated using the formula $\sigma = F/A$, $\varepsilon = D/h*100\%$, where F is the force when fracture, and A is the cross-sectional area of the sample. D is the displacement fracture, and h is the initial height between the clamps. To test the self-recovery properties, the C/P(AAm-AAc)/ Fe^{3+} hydrogel was first stretched to a preset deformation of 400% and then unloaded. This process was repeated 5 times to make the hydrogel fatigue enough. Then the hydrogel was placed under room temperature or sunlight or Xenon lamp (CEL-HXF300, AuLight, China) of 1 kW m⁻² (simulated 1 sun) for 15 or 30 min, and the sixth cycle stretching was repeated once under the same deformation to calculate the ratio of the dissipated energy after recovery to the dissipated energy in the first load-unload cycle to indicate the self-recovery efficiency.

1.3.2 Self-healing. The hydrogel was cut in half, and then the two sections of hydrogels were placed in a mold, making sure that their cuts fitted snugly together. The sample is sealed with plastic wrap to prevent dehydration of the hydrogels. After sealing, it was then placed in an oven of 55 °C or at room temperature or Xenon lamp of 1

kW m^{-2} (simulated 1 sun) or real sunlight for 1–8 hours for self-healing. The self-healing efficiency was calculated by dividing the tensile fracture strength of the sample after healing by the tensile fracture strength of the original sample.

1.3.3 Photothermal performance test. The temperature of the hydrogel surface was observed using a thermal imager (FLIR A300-Series, FLIR, Sweden). The temperature of hydrogels was recorded every five minutes. During the test, hydrogels were wrapped with plastic wraps to prevent evaporation of water.

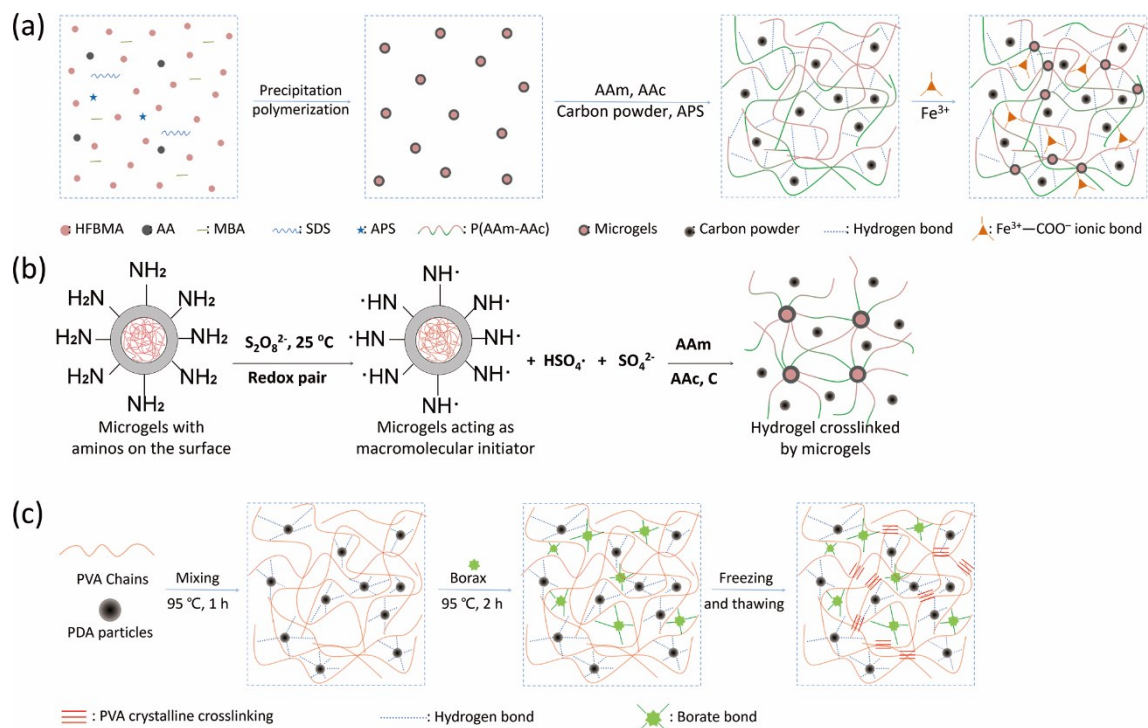


Fig. S1 Synthesis diagrams: (a) C/P(AAm-AAc)/Fe³⁺, (b) the cross-linking mechanism of C/P(AAm-AAc)/Fe³⁺ hydrogel, (c) PVA/PDA/Borax hydrogel.

C/P(AAm-AAc)/Fe³⁺ was soaked in water, 0.1 mol/L EDTA-2Na solution and 0.5 mol/L urea solution for 140 h, respectively. The swelling curves and photos after swelling were recorded. As shown in Fig. S2a, the swelling rate of C/P(AAm-AAc)/Fe³⁺ in the above three solutions are obviously different. As shown in Fig. S2b, the C/P(AAm-AAc)/Fe³⁺ sample soaked in EDTA-2Na solution cannot maintain its original shape with an extremely low modulus. This is because the ionic bond of the sample was broken in the EDTA-2Na solution. However, the covalent bonds still exist as the sample was not completely dissolved. The swelling ratio of C/P(AAm-AAc)/Fe³⁺ after soaking in urea solution is larger than that after soaking in water. It is owing to that the hydrogen bond of the sample is destroyed in the urea solution, which leads to a decreased crosslinking degree of the sample. All these results indicate that C/P(AAm-AAc)/Fe³⁺ contains covalent bond crosslinking, ionic bond crosslinking, and hydrogen bond crosslinking.

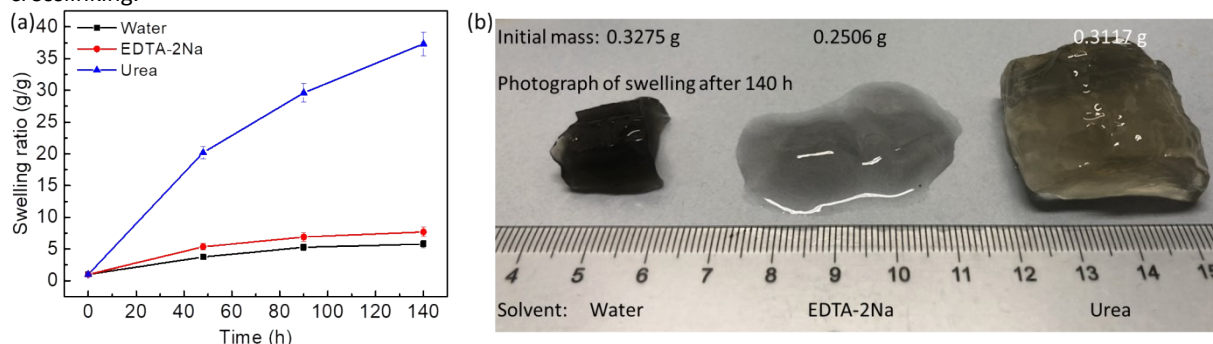


Fig. S2 (a) Swelling curves of C/P(AAm-AAc)/Fe³⁺ hydrogels swelled in different solvents and (b) digital photos after swelling for 140 h.

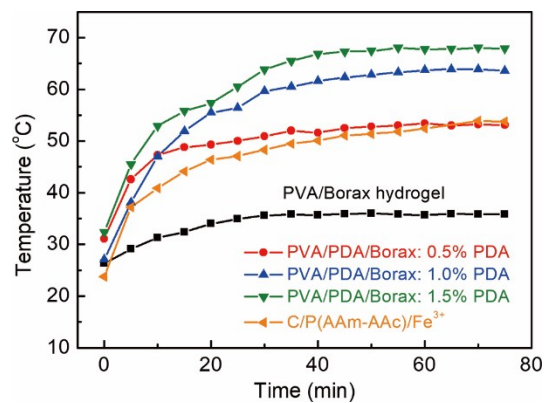


Fig. S3 The temperature rises of PVA/PDA/Borax and C/P(AAm-AAc)/Fe³⁺ hydrogels under simulated sunlight.

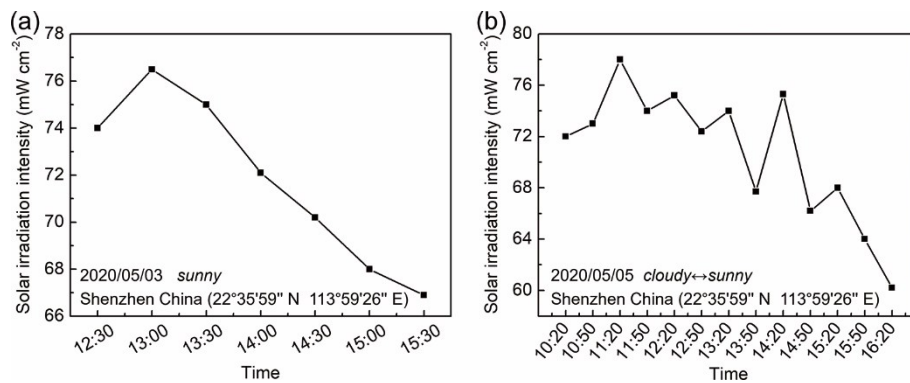


Fig. S4 The actual sunlight irradiation intensity during wound self-healing test: (a) PVA/PDA/Borax hydrogel, (b) C/P(AAm-AAC)/Fe³⁺ hydrogel.

To explore the effect of reversible ionic crosslinking on the self-healing properties, C/P(AAm-AAc) hydrogel was immersed in 0.05 mol/L ferric chloride solution with different time to obtain C/P(AAm-AAc)/Fe³⁺ hydrogels with different degree of ionic crosslinking. As shown in Fig. S5a and b, they are the tensile stress-strain curves of the original C/P(AAm-AAc)/Fe³⁺ hydrogels and the broken sample after 6 h of self-healing under simulated sunlight. As the soaking time increased from 10 min to 30 min, the breaking strength and elongation at break of hydrogels increases with time. This is due to the too few crosslinks within 30 min. However, with the prolongation of immersion time, the breaking strength and elongation at break of hydrogels is decreased after self-healing. This may be due to prolonged immersion in the hydrogel resulting in excessive Fe³⁺, which makes Fe³⁺ and carboxylic acid more likely to form mono-, bidentates than tridentates, resulting in its mechanical properties reduced. When the soaking time is 30 min, the breaking strength and elongation at break of the hydrogel reached the maximum value of approximately 140 kPa and 500% respectively. Thus, the optimum ionic immersion time of 30 min for self-healing is determined.

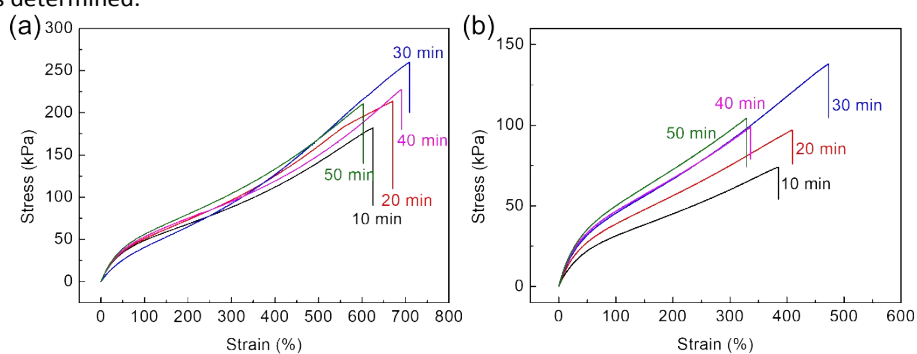


Fig. S5 Effect of immersion time in FeCl₃ of 0.05 mol/L on mechanical properties of C/P(AAm-AAc)/Fe³⁺ hydrogel: (a) original sample, (b) self-healed sample.

To test the effect of photothermal effect on the self-healing of hydrogels, the cut-in-two C/P(AAm-AAC)/Fe³⁺ hydrogels were placed under simulated sunlight for different time. The healing samples were subjected to uniaxial tension until the fracture occurred to measure the healing performance. As shown in Fig. S6a, the breaking strength and elongation at break of the initial C/P(AAm-AAC)/Fe³⁺ hydrogel are 260 kPa and 710% respectively. The self-healing efficiency is gradually increased with time from 1 h to 6 h as the fracture strength and elongation at break increased, which is consistent with the result of wound self-healing under actual sunlight. But, compare with the stress-strain curves of 6 h and 8 h, there is little difference between their fracture strengths and elongations at break. Their fracture strengths are approximately 52% of the initial strength, and the elongations are approximately 67% of the initial sample. Neither of them has recovered to 100%. This is because when the hydrogel is cut off, not only the reversible non-covalent interactions are destroyed, but also some chemical bonds who are not healing are destroyed. This also shows that the time of 6 h is enough to fully recover the reversible physical crosslinking in C/P(AAm-AAC)/Fe³⁺ hydrogel. By comparing the difference in the self-healing efficiency of PVA/PDA/Borax hydrogel and C/P(AAm-AAC)/Fe³⁺ hydrogel, the recovery efficiency of PVA/PDA/Borax hydrogel is significantly higher. This is because the cross-linking methods in PVA/PDA/Borax hydrogel are all reversible interactions. Under the irradiation of 1 sun illumination, the raised temperature gives the material a certain plasticity. However, in the case of C/P(AAm-AAC)/Fe³⁺ hydrogel, the inherent chemical crosslinking cannot be recovered after being cut. It can also be seen that when the healing time is 1 h under simulated sunlight, the breaking strength of the hydrogel has exceeded 50 kPa already, which is greater than that of self-healing at room temperature for 6 h as shown in Fig. S6b showing that the photothermal effect greatly promotes the self-healing performance.

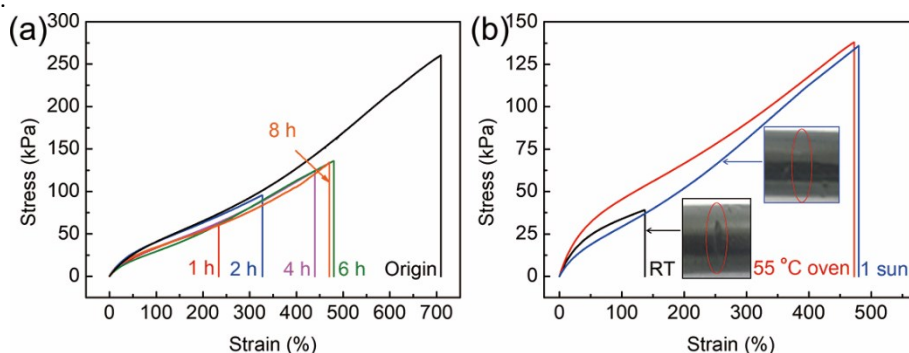


Fig. S6 (a) The tensile stress-strain curves of as-prepared C/P(AAm-AAC)/Fe³⁺ hydrogel and self-healing cut-in-two C/P(AAm-AAC)/Fe³⁺ hydrogel at different times under simulated sunlight. (b) The self-healing of C/P(AAm-AAC)/Fe³⁺ hydrogel under room temperature, 55 °C oven and simulated sunlight for 6 h.

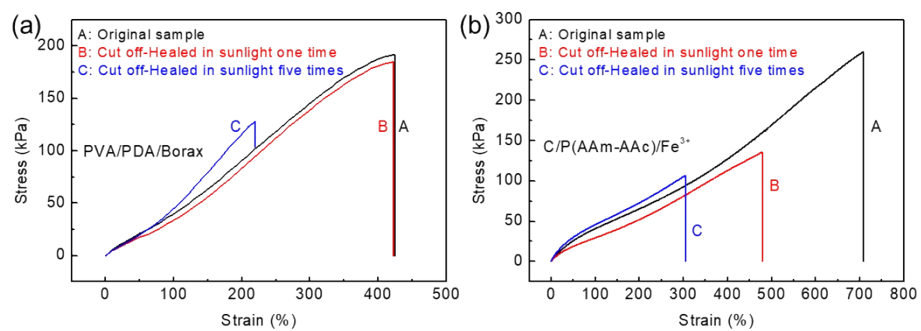


Fig. S7 The tensile fracture curves of the original sample, the sample after one cut-healed cycle, and the sample after five cut-healed repeating cycles: (a) PVA/PDA/Borax hydrogel (Borax: 3.0%; PDA: 1.5%; F-T-3; healing time: 3 h), (b) C/P(AAm-AAc)/Fe³⁺ hydrogel (healing time: 6 h).

Table S1 The collations and comparisons of self-repair research results reported in the literature compared from materials, healing mechanisms, healing conditions, efficiency and speed of self-healing and published years.

Materials	Type of reversible interactions	Conditions or stimuli	Efficiency of self-healing or self-recovery ^a	Published year	Ref.
Poly(vinyl alcohol) hydrogel	hydrogen bonds	25 °C	self-healing: 72% in 48 h	2012	4
Cyclodextrins host and aliphatic guest hydrogel	host-guest supramolecular interaction	25 °C, wet condition	self-healing: 74% in 24 h of α CD- <i>n</i> Bu gel; 99% in 24 h of β CD-Ad gel	2013	5
Graphene oxide composite hydrogel	interactions between the polymer chains and the GO sheets	30 °C	self-healing: 88% in 24 h	2013	6
Polyampholyte hydrogel: P(NaSS-co-DMAEA-Q) 2.0-0.52	charge combinations	25 °C, water	self-healing: 99% in 24 h self-recovery: 100% in 2 h	2013	7
Poly(acrylic acid) hydrogel	hydrophobic interactions	80 °C, solutions of various pH's containing CTAB and NaBr	self-healing: 75% in 30 min	2014	8
PAA/PAH polyelectrolyte complexes	interfusion of the polyelectrolyte chains	120 °C, 1 mol L ⁻¹ NaCl	self-healing: 100% in 8 h	2014	9
Graphene/Clay/Poly (<i>N,N</i> -dimethylacrylamide)	interaction between the polymer chains and the clay platelets	808 nm NIR light	self-healing: 96% in 3 min	2014	10
AgNWs/PCL/PVA	thermoplasticity of PCL/PVA	812 nm NIR light	conductivity self-healing: 94% in 2.5 min	2014	11
Agar/HPPAAm DN gel	hydrophobic associations	25 °C	self-healing: 40% in 24 h	2015	12
Covalent network polymer	dynamic boronic ester bonds	50 °C	self-healing: ~100% in 16 h	2015	13
Supramolecular polymer hydrogel	dual amide hydrogen bonds	90 °C	self-healing: ~100% in 12 h	2015	14
Boronic acid-based hydrogel	borate bonds	neutral and acidic pH	self-healing: support own weight in 60 min	2015	15
PEG based self-healing hydrogel	borate bonds	25 °C	self-healing: support own weight in 30 min	2015	16

PVA-PEG DN hydrogel	hydrogen bonds	25 °C	self-healing: 68% in 48 h	2015	17
(PAM-co-PAA)/PVA hydrogel	hydrogen bonds	37 °C	self-healing: 35% in 12 h	2016	18
Poly(acrylamide-co-acrylic acid) hydrogel	hydrogen bonds, ionic bonds	25 °C	self-recovery: 65% in 4 h	2016	19
PVA hybrid hydrogel	metal-ligand coordination, hydrogen bonds	25 °C	self-healing: 86.8% in 12 h	2016	20
UPyHCBA-based gel	SDS reconfiguration, humidity	25 °C	self-healing: ~80% in 30 s	2016	21
Supramolecular guest-host hydrogel	supramolecular interactions	25 °C, aqueous conditions	self-recovery: 90% in 6 s	2016	22
Ternarily crosslinked nanocomposite physical hydrogel	hydrophobic interactions, hydrogen bonds	80 °C	self-healing: ~72% in 24 h	2016	23
mPDAP/Poly(ϵ -caprolactone)	melting-recrystallization	808 nm NIR light	self-healing: ~100% in 30 s	2016	24
Au@PCL/rGO/AgNWs	melting of crystalline PCL chains	532 nm light	conductivity self-healing: 91% in 5 min	2016	25
TetraPEG DYNA gel	dynamic covalent networks	acidic conditions	self-healing: support own weight in 48 h	2017	26
Elastomeric hydrogel	borate ester bonds	25 °C	self-healing: ~100% in 48 h	2017	27
Carboxymethyl cellulose-based hydrogel	ionic coordination between Al ³⁺ and COO ⁻	25 °C	self-healing: 95% in 48 h	2017	28
Doubly dynamic self-healing hydrogel	oxime click chemistry, boronic bonds	25 °C	self-healing: support own weight in 3 h	2017	29
Physically crosslinked DN hydrogel	Fe ³⁺ coordination, hydrogen bonds	25 °C	self-recovery: ~100% in 60 min	2017	30
		Fe ³⁺ solution	self-recovery: ~100% in 30 min		
		50 °C	self-recovery: ~100% in 15 min		
		25 °C	self-healing: 25% in 60 h		
NH ₂ -MWCNTs/DA-epoxy	Diels-Alder reaction	NIR	self-healing: 77% in 5 min	2017	31

Graphene/Polyurethane	Diels–Alder reaction	980 nm NIR light	self-healing: 96% in 1 min	2017	32
CNT/SBS elastomer	Diels–Alder reaction	808 nm NIR light	self-healing: ~100% in 10 s	2017	33
Oligoaniline-modified vitrimers	thermoplasticity of vitrimers	808 nm NIR light	self-healing: ~100% in 5 s	2017	34
Fe ₃ O ₄ /TPU	thermoplasticity of PU	IR light	self-healing: cracks disappeared in 20 s	2017	35
KC/PAM DPC-DN hydrogel	hydrophobic association, K ⁺ -induced helices bundle formation	25 °C	self-recovery: ~100% in 2 min	2018	36
		70 °C	self-healing: 49% in 24 h		
PAA-Fe ³⁺ /CS DN hydrogel	metal-coordination, chain entanglement	70 °C	self-healing: 37% in 24 h	2018	37
CS-Ca ²⁺ /PAA-Fe ³⁺ DN hydrogel	two distinct coordination, chain entanglement	70 °C	self-healing: 19% in 24 h	2018	38
BSA/Epichlorohydrin hydrogel	hydrogen bonds, viscoelastic nature	25 °C	self-healing: support own weight in 24 h	2018	39
PVA hydrogel	electrostatic interactions	254 nm UV illumination, 25 °C	self-healing: conductive in 2 h	2018	40
rmGO/AgNWs/Polyurethane	Diels–Alder reaction	808 nm NIR light (20 min) 65 °C (48 h)	self-healing: ~90% in 48 h 20 min	2018	41
BN/PDA/PBO	thermoplasticity of polyurethane droplets	Xenon light	self-healing: 73% in 150 min	2018	42
LBG/Gg DN hydrogel	hydrogen bonds, borate bonds	80 °C	self-healing: ~100% in 30 min	2019	43
DCN hydrogel	diol–benzoxaborolate	25 °C	self-healing: support own weight in 3 s	2019	44
(PAAm)/chitosan (CS) hybrid hydrogel	hydrophobic associations	25 °C	self-healing: ~100% in 30 min	2019	45
(UPy)-based supramolecular polymer	photothermal effect of carbon nanotubes	808 nm NIR light	self-healing: cracks disappeared in 90 s	2019	46
PAM/PVA PDN hydrogel	hydrogen bonds, hydrophobic associations	60 °C	self-healing: cracks disappeared in 5 h	2019	47

PVA/PDA/Borax	hydrogen bonds, borate bonds	sunlight	self-healing: over 96% in 3 h	/	Our work
C/P(AAm-AAc)/Fe ³⁺	hydrogen bonds, ionic bonds	sunlight	self-recovery: 94% in 30 min	/	Our work

^a The efficiency of self-healing or self-recovery is calculated from fracture tensile stress.

References

- 1 X. Liang, Y. Deng, X. Pei, K. Zhai, K. Xu, Y. Tan, X. Gong and P. Wang, *Soft Matter*, 2017, **13**, 2654.
- 2 L. Yang, Z. Wang, G. Fei and H. Xia, *Macromol. Rapid. Comm.*, 2017, **38**, 1700421.
- 3 Y. Liu, K. Ai, J. Liu, M. Deng, Y. He and L. Lu, *Adv. Mater.*, 2013, **25**, 1353.
- 4 H. Zhang, H. Xia and Y. Zhao, *ACS Macro Lett.*, 2012, **1**, 1233.
- 5 T. Kakuta, Y. Takashima, M. Nakahata, M. Otsubo, H. Yamaguchi and A. Harada, *Adv. Mater.*, 2013, **25**, 2849.
- 6 J. Liu, G. Song, C. He and H. Wang, *Macromol. Rapid. Comm.*, 2013, **34**, 1002.
- 7 T. L. Sun, T. Kurokawa, S. Kuroda, A. B. Ihsan, T. Akasaki, K. Sato, M. A. Haque, T. Nakajima and J. P. Gong, *Nat. Mater.*, 2013, **12**, 932.
- 8 U. Gulyuz and O. Okay, *Macromolecules*, 2014, **47**, 6889.
- 9 A. Reisch, E. Roger, T. Phoeung, C. Antheaume, C. Orthlieb, F. Boulmedais, P. Lavalley, J. B. Schlenoff, B. Frisch and P. Schaaf, *Adv. Mater.*, 2014, **26**, 2547.
- 10 E. Zhang, T. Wang, L. Zhao, W. Sun, X. Liu and Z. Tong, *ACS Appl. Mater. Interfaces*, 2014, **6**, 22855.
- 11 Y. Li, S. Chen, M. Wu and J. Sun, *ACS Appl. Mater. Interfaces*, 2014, **6**, 16409.
- 12 Q. Chen, L. Zhu, H. Chen, H. Yan, L. Huang, J. Yang and J. Zheng, *Adv. Funct. Mater.*, 2015, **25**, 1598.
- 13 O. R. Cromwell, J. Chung and Z. Guan, *J. Am. Chem. Soc.*, 2015, **137**, 6492.
- 14 X. Dai, Y. Zhang, L. Gao, T. Bai, W. Wang, Y. Cui and W. Liu, *Adv. Mater.*, 2015, **27**, 3566.
- 15 C. C. Deng, W. L. A. Brooks, K. A. Abboud and B. S. Sumerlin, *ACS Macro Lett.*, 2015, **4**, 220.
- 16 L. He, D. Szopinski, Y. Wu, G. A. Luinstra and P. Theato, *ACS Macro Lett.*, 2015, **4**, 673.
- 17 G. Li, H. Zhang, D. Fortin, H. Xia and Y. Zhao, *Langmuir*, 2015, **31**, 11709.
- 18 Z. Gong, G. Zhang, X. Zeng, J. Li, G. Li, W. Huang, R. Sun and C. Wong, *ACS Appl. Mater. Interfaces*, 2016, **8**, 24030.
- 19 Y. Hu, Z. Du, X. Deng, T. Wang, Z. Yang, W. Zhou and C. Wang, *Macromolecules*, 2016, **49**, 5660.
- 20 Y. Hui, Z.-B. Wen, F. Pilate, H. Xie, C.-J. Fan, L. Du, D. Liu, K.-K. Yang and Y.-Z. Wang, *Polym. Chem.*, 2016, **7**, 7269.
- 21 I. Jeon, J. Cui, W. R. Illeperuma, J. Aizenberg and J. J. Vlassak, *Adv. Mater.*, 2016, **28**, 4678.
- 22 C. B. Rodell, N. N. Dusaj, C. B. Highley and J. A. Burdick, *Adv. Mater.*, 2016, **28**, 8419.
- 23 F.-K. Shi, M. Zhong, L.-Q. Zhang, X.-Y. Liu and X.-M. Xie, *J. Mater. Chem. B*, 2016, **4**, 6221.
- 24 S. Xiong, Y. Wang, J. Zhu, J. Yu and Z. Hu, *Polymer*, 2016, **84**, 328.
- 25 L. Chen, L. Si, F. Wu, S. Y. Chan, P. Yu and B. Fei, *J. Mater. Chem. C*, 2016, **4**, 10018.
- 26 D. E. Apostolides, T. Sakai and C. S. Patrickios, *Macromolecules*, 2017, **50**, 2155.
- 27 Y. Chen, W. Qian, R. Chen, H. Zhang, X. Li, D. Shi, W. Dong, M. Chen and Y. Zhao, *ACS Macro Lett.*, 2017, **6**, 1129.
- 28 Y. M. Chen, L. Sun, S. A. Yang, L. Shi, W. J. Zheng, Z. Wei and C. Hu, *Eur. Polym. J.*, 2017, **94**, 501.
- 29 J. Collins, M. Nadgorny, Z. Xiao and L. A. Connal, *Macromol. Rapid. Comm.*, 2017, **38**, 1600760.
- 30 X. Li, Q. Yang, Y. Zhao, S. Long and J. Zheng, *Soft Matter*, 2017, **13**, 911.
- 31 Q.-T. Li, M.-J. Jiang, G. Wu, L. Chen, S.-C. Chen, Y.-X. Cao and Y.-Z. Wang, *ACS Appl. Mater. Interfaces*, 2017, **9**, 20797.
- 32 S. Wu, J. Li, G. Zhang, Y. Yao, G. Li, R. Sun and C. Wong, *ACS Appl. Mater. Interfaces*, 2017, **9**, 3040.
- 33 J. Bai and Z. Shi, *ACS Appl. Mater. Interfaces*, 2017, **9**, 27213.
- 34 Q. Chen, X. Yu, Z. Pei, Y. Yang, Y. Wei and Y. Ji, *Chem. Sci.*, 2017, **8**, 724.
- 35 X. Yin, Y. Zhang, P. Lin, Y. Liu, Z. Wang, B. Yu, F. Zhou and Q. Xue, *J. Mater. Chem. A*, 2017, **5**, 1221.
- 36 Y. Deng, M. Huang, D. Sun, Y. Hou, Y. Li, T. Dong, X. Wang, L. Zhang and W. Yang, *ACS Appl. Mater. Interfaces*, 2018, **10**, 37544.
- 37 X. H. Wang, F. Song, D. Qian, Y. D. He, W. C. Nie, X. L. Wang and Y. Z. Wang, *Chem. Eng. J.*, 2018, **349**, 588.
- 38 X.-H. Wang, F. Song, J. Xue, D. Qian, X.-L. Wang and Y.-Z. Wang, *Polymer*, 2018, **153**, 637.
- 39 A. Upadhyay, R. Kandi and C. P. Rao, *ACS Sustainable Chem. Eng.*, 2018, **6**, 3321.
- 40 D. Yang, Y. Wang, Z. Li, Y. Xu, F. Cheng, P. Li and H. Li, *J. Mater. Chem. C*, 2018, **6**, 1153.
- 41 C. Lin, D. Sheng, X. Liu, S. Xu, F. Ji, L. Dong, Y. Zhou and Y. Yang, *Polymer*, 2018, **140**, 150.
- 42 Q. Shao, Z. Hu, X. Xu, L. Yu, D. Zhang and Y. Huang, *Appl. Surf. Sci.*, 2018, **440**, 1159.
- 43 Y. Lv, Z. Pan, C. Song, Y. Chen and X. Qian, *Soft Matter*, 2019, **15**, 6171.
- 44 D. Wu, W. Wang, D. Diaz-Dussan, Y.-Y. Peng and D. G. Hall, *Chem. Mater.*, 2019, **31**, 4092.
- 45 S. Xia, S. Song, F. Jia and G. Gao, *J. Mater. Chem. B*, 2019, **7**, 4638.
- 46 B. Li, L. Kan, S. Zhang, Z. Liu, C. Li, W. Li, X. Zhang, H. Wei and N. Ma, *Nanoscale*, 2019, **11**, 467.
- 47 L. Xing, C. Hu, Y. Zhang, X. Wang and R. Ran, *J. Mater. Sci.*, 2019, **54**, 3368.